Transport in Porous Media **49:** 41–58, 2002.

Localization of Mean Flow and Apparent Transmissivity Tensor for Bounded Randomly Heterogeneous Aquifers

DANIEL M. TARTAKOVSKY[1], ALBERTO GUADAGNINI[2], FRANCESCO BALLIO[2] and ALEXANDRE M. TARTAKOVSKY[3]
[1]*Theoretical Division, Los Alamos National Laboratory, U.S.A. e-mail: dmt@lanl.gov*
[2]*D.I.I.A.R. – Politecnico di Milano, Italy. e-mail: alberto.guadagnini@polimi.it*
[3]*Department of Hydrology and Water Resources, University of Arizona, U.S.A. e-mail: sasha@hwr.arizona.edu*

(Received: 15 November 2000; in final form: 18 December 2001)

Abstract. We explore the concept of apparent transmissivity for bounded randomly heterogeneous media under steady-state flow regime. The novelty of our study consists of investigating a tensorial nature of apparent transmissivity. We demonstrate that apparent transmissivity of bounded domains is anisotropic even though an underlying local transmissivity field is statistically isotropic. For rectangular flow domains, we derive an analytical expression for the apparent transmissivity tensor via localization and perturbation expansion of the nonlocal mean flow equations in the variance of log-transmissivity. In this expression, almost everywhere the off-diagonal terms are several orders of magnitude smaller than the diagonal terms. When the domain size relative to the log-transmissivity correlation scale is large, the longitudinal and transverse components of the apparent transmissivity tensor approach the geometric mean of local transmissivity. While rigorously valid for mean uniform flows only, our expression for the apparent transmissivity tensor leads to mean hydraulic head distributions that compare favorably with those obtained through Monte-Carlo simulations and the nonlocal mean flow equations even in the presence of pumping wells. This agreement deteriorates in the vicinity of wells and as pumping rates increase.

Key words: stochastic, effective, equivalent, conductivity, perturbation.

Nomenclature

d	space dimension.
$\mathcal{E}$	relative errors.
G	Green's function.
h	hydraulic head.
$\mathbf{I}$	identity tensor.
$\mathbf{J}$	mean hydraulic gradient.
l_Y	correlation scale of Y.
$\mathbf{q}$	Darcy flux.
Q	pumping flow rate.
$\mathbf{r}$	residual flux (mixed ensemble moment).
T	transmissivity.
$\mathbf{T}_{ap}$	apparent transmissivity tensor.

T_{ef}	effective transmissivity.
T_g	geometric mean of transmissivity.
T_h	harmonic mean of transmissivity.
T_{ij}	components of the apparent transmissivity tensor.
$\mathbf{x}$	coordinate vector.
X	generic random field.
$\bar{X}$	ensemble mean of X.
X'	zero-mean fluctuations about $\bar{X}$.
Y	log-transmissivity, $Y = \ln T$.
ϵ	geometric factor.
λ	relative correlation scale.
Ω	flow domain.
ρ_Y	correlation function of Y.
σ_Y^2	variance of Y.

1. Introduction

Macroscopic description of flow of fluids through porous media relies on Darcy's law, $\mathbf{q}(\mathbf{x}) = -T(\mathbf{x})\nabla h(\mathbf{x})$, where $\mathbf{q}$ is the Darcy flux and h is the hydraulic head. Parameters, such as medium transmissivity $T(\mathbf{x})$, were traditionally viewed as well-defined local quantities that can be assigned unique values at each point in space. Yet in practice they are deduced from measurements at selected locations and depth intervals, where their values depend on the scale and mode of measurement. Quite often, the measurement support is uncertain and data are corrupted by experimental and interpretative errors. Estimating the parameters at points where measurements are not available entails additional errors. Hence, it might be appropriate to describe transmissivity, $T(\mathbf{x})$, as a random field. Yet, the tradition has been to model subsurface flow deterministically. One of the most significant conceptual difficulties in applying traditional deterministic flow models stems from for the apparent scale dependence of hydraulic properties of natural aquifers (Gelhar, 1993; Neuman, 1994).

It is often computationally expedient to replace spatially varying (random) local transmissivity, $T(\mathbf{x})$, with their effective counterparts, T_{ef}. Effective transmissivity, T_{ef}, is defined as a coefficient of proportionality between the ensemble mean flux, $\bar{\mathbf{q}}(\mathbf{x})$, and the ensemble mean head gradient, $\nabla\bar{h}(\mathbf{x})$,

$$\bar{\mathbf{q}}(\mathbf{x}) = -T_{ef}\nabla\bar{h}(\mathbf{x}). \tag{1}$$

For mean uniform flows ($\nabla\bar{h} = \text{const}$) in statistically homogeneous and isotropic infinite domains, effective transmissivity T_{ef} is a characteristic of the medium only. It is given by the harmonic, T_h, and geometric, T_g, means of $T(\mathbf{x})$ in one and two dimensions, respectively (Matheron, 1967; Dagan, 1989, Equation 3.4.62).

The situation changes when flow becomes non-uniform in the mean, and/or boundaries of a flow domain are introduced. Under these conditions, T_{ef} depends not only on the medium properties, but also on the flow regime (Sànchez-Vila,

1997 and references therein). To make this distinction clear, Indelman *et al.* (1996) used the terms 'equivalent' or 'apparent' transmissivity, $\mathbf{T}_{ap}$, rather than 'effective'. Even when an underlying transmissivity field is statistically isotropic, the corresponding equivalent transmissivity might be anisotropic (Neuman and Orr, 1993; Tartakovsky *et al*., 1999).

In this paper we investigate the meaning of hydrogeologic parameters, that enter into traditional deterministic groundwater flow models, when these parameters are used to describe (randomly) heterogeneous media. This is done by localizing the nonlocal mean flow equations and introducing apparent transmissivity. The latter is revealed to be a tensorial quantity, whose nature is explored in detail. Reliance on transmissivity rather than hydraulic conductivity restricts our results to two-dimensional, predominantly horizontal flows. However, the theory and analysis can be readily extended to three-dimensional flow scenarios. For an in-depth investigation of the relationship between the statistics of hydraulic conductivity and transmissivity, we refer the interested reader to Tartakovsky *et al*. (2000).

2. Non-Darcian Mean Fluxes and Their Localization

In general, for non-uniform (in the mean) flows in bounded aquifers neither effective nor apparent transmissivities exist (Neuman and Orr, 1993). Instead, Equation (1) is replaced with a non-Darcian equation (Neuman and Orr, 1993; Neuman *et al*., 1996),

$$\bar{\mathbf{q}}(\mathbf{x}) = -\bar{T}\,\nabla\bar{h}(\mathbf{x}) + \mathbf{r}(\mathbf{x}), \tag{2}$$

where $\bar{T}$ is the ensemble mean of T and $\mathbf{r}(\mathbf{x}) = -\overline{T'(\mathbf{x})\nabla h'(\mathbf{x})}$ is the 'residual' dispersive flux representing the cross-covariance between the transmissivity and hydraulic gradient fluctuations. (Here we use the Reynolds decomposition to represent a random field X as the sum of its mean $\bar{X}$ and zero-mean fluctuations X' about this mean.) The latter can be found as the solution of an integral equation

$$\mathbf{r}(\mathbf{x}) = \int_\Omega \mathbf{a}(\mathbf{y}, \mathbf{x})\,\nabla\bar{h}(\mathbf{y})\,\mathrm{d}\mathbf{y} + \int_\Omega \mathbf{b}(\mathbf{y}, \mathbf{x})\,\mathbf{r}(\mathbf{y})\,\mathrm{d}\mathbf{y}, \tag{3}$$

where Ω is a flow domain, and $\mathbf{a}$ and $\mathbf{b}$ are symmetric positive-semidefinite and non-symmetric dyadics, respectively. It follows from Equations (2) and (3) that mean flux $\mathbf{q}(\mathbf{x})$ is nonlocal, that is, depends on head gradients at points other than $\mathbf{x}$ (see also Dagan, 1989; Cushman, 1997, §3.4.6).

For apparent transmissivity to exist in the strict sense, it is necessary that $\nabla\bar{h}$ and $\mathbf{r}$ be constant. Dagan (1982) considered a less restrictive scenario where $\nabla\bar{h}$ varies slowly in space and time, that is, has negligibly small space and time derivatives. Tartakovsky and Neuman (1998c) investigated the errors introduced by temporal localization. If both $\nabla\bar{h}$ and $\mathbf{r}$ vary slowly in space, one can approximate Equation (3) through the localization

$$\mathbf{r}\,(\mathbf{x}) \approx \mathbf{A}\,(\mathbf{x})\nabla\bar{h}\,(\mathbf{x}) + \mathbf{B}\,(\mathbf{x})\,\mathbf{r}\,(\mathbf{x}), \tag{4a}$$

where

$$\mathbf{A}(\mathbf{x}) = \int_\Omega \mathbf{a}(\mathbf{y}, \mathbf{x})\, d\mathbf{y} \quad \text{and} \quad \mathbf{B}(\mathbf{x}) = \int_\Omega \mathbf{b}(\mathbf{y}, \mathbf{x})\, d\mathbf{y}. \tag{4b}$$

Then

$$\mathbf{r}(\mathbf{x}) \approx \mathbf{t}(\mathbf{x})\nabla\bar{h}(\mathbf{x}), \tag{5a}$$

where $\mathbf{t}$ is a non-symmetric second-rank tensor

$$\mathbf{t}(\mathbf{x}) = [\mathbf{I} - \mathbf{B}(\mathbf{x})]^{-1}\mathbf{A}(\mathbf{x}), \tag{5b}$$

$\mathbf{I}$ being the identity tensor. Substituting Equation (5) into Equation (2) yields an approximate form of the mean Darcy's law

$$\bar{\mathbf{q}}(\mathbf{x}) \approx -\mathbf{T}_{ap}(\mathbf{x})\nabla\bar{h}(\mathbf{x}), \tag{6}$$

where the spatially varying apparent transmissivity tensor is given by

$$\mathbf{T}_{ap}(\mathbf{x}) = \bar{T}\mathbf{I} - \mathbf{t}(\mathbf{x}). \tag{7}$$

Thus the localization (4a) of the mean flow equations yields a deterministic system of differential equations, which is identical in form to traditional flow equations commonly written for fully deterministic media with transmissivity (7).

Practical evaluation of the apparent transmissivity tensor (7) requires a closure approximation for Equation (4b). Such a closure is commonly derived through perturbation expansions of $\mathbf{a}$ and $\mathbf{b}$ in a small parameter $\sigma_Y^2 < 1$, variance of log transmissivity $Y(\mathbf{x}) = \ln T(\mathbf{x})$. This requirement implies that porous media are *mildly* heterogeneous. However, the resulting expressions can be made applicable for highly heterogeneous media by means of a relatively straightforward generalization (e.g. Paleologos *et al.*, 1996).

3. Perturbation Expansions

Consider asymptotic expansions of parameters and functions, $\bar{T} = T_g(1 + \sigma_Y^2/2 + \cdots)$; $\bar{\mathbf{q}} = \bar{\mathbf{q}}^{(0)} + \bar{\mathbf{q}}^{(1)} + \cdots$; $\bar{h} = \bar{h}^{(0)} + \bar{h}^{(1)} + \cdots$; and $\mathbf{r} = \mathbf{r}^{(1)} + \cdots$, where $T_g = \exp(\bar{Y})$, $\bar{Y}$ being the ensemble mean of Y. The superscript (i) denotes terms that are of ith-order, that is, contain only the ith power of σ_Y^2. It follows from Equations (4a) and (4b) that the first-order (in σ_Y^2) approximation of the localized residual flux $\mathbf{r}$ is given by $\mathbf{r}^{(1)} = \mathbf{A}^{(1)}\nabla\bar{h}^{(0)}$, where (Tartakovsky and Neuman, 1998b; Guadagnini and Neuman, 1999a)

$$\mathbf{A}^{(1)}(\mathbf{x}) = \int_\Omega \mathbf{a}^{(1)}(\mathbf{y}, \mathbf{x})\, d\mathbf{y} \tag{8a}$$

and

$$\mathbf{a}^{(1)}(\mathbf{y}, \mathbf{x}) = T_g\sigma_Y^2\rho_Y(\mathbf{y}, \mathbf{x})\nabla_{\mathbf{x}}\nabla_{\mathbf{y}}^T G(\mathbf{y}, \mathbf{x}). \tag{8b}$$

Here $\rho_Y(\mathbf{y}, \mathbf{x})$ is the spatial two-point correlation function of Y, and $G(\mathbf{y}, \mathbf{x})$ is the deterministic Green's function for Laplace equation in Ω subject to the appropriate homogeneous boundary conditions.

Collecting the terms of the same powers of σ_Y^2 yields the zeroth-order approximation of mean flux in Equation (2)

$$\bar{\mathbf{q}}^{(0)}(\mathbf{x}) = -T_g \nabla \bar{h}^{(0)}(\mathbf{x}), \tag{9}$$

and its first-order approximation

$$\bar{\mathbf{q}}^{(1)}(\mathbf{x}) = -T_g \left[\nabla \bar{h}^{(1)}(\mathbf{x}) + \frac{\sigma_Y^2}{2} \nabla \bar{h}^{(0)}(\mathbf{x}) \right] + \mathbf{r}^{(1)}(\mathbf{x}). \tag{10}$$

Strictly speaking, for such expansions to be asymptotic, it is necessary that $\sigma_Y^2 \ll 1$. However, various numerical simulations (e.g. Guadagnini and Neuman, 1999b) demonstrated that these first-order approximations remain remarkably robust even for strongly heterogeneous media with σ_Y^2 as large as 4.

When the mean flow equations can be localized, retaining the two leading terms in the asymptotic expansion of $\bar{\mathbf{q}}$ in (2), $\bar{\mathbf{q}} \approx \bar{\mathbf{q}}^{[1]} \equiv \bar{\mathbf{q}}^{(0)} + \mathbf{q}^{(1)}$, yields

$$-\frac{\bar{\mathbf{q}}^{[1]}(\mathbf{x})}{T_g} = \nabla \bar{h}^{(1)}(\mathbf{x}) + \left[\left(1 + \frac{\sigma_Y^2}{2} \right) \mathbf{I} - \hat{\mathbf{A}}^{(1)}(\mathbf{x}) \right] \bar{\mathbf{J}}(\mathbf{x}), \tag{11}$$

where the superscript in angular brackets defines the order of the expansion, $\hat{\mathbf{A}}^{(1)} = T_g^{-1}\mathbf{A}^{(1)}$ and $\bar{\mathbf{J}} = \nabla \bar{h}^{(0)}$. For flow through infinite, statistically homogeneous porous media under mean uniform flow conditions, the mean hydraulic head gradient $\bar{\mathbf{J}} = \text{const.}$ and $\nabla \bar{h}^{(i)} = 0$, $i \geqslant 1$ (Dagan, 1989, §3.4.2). Under these conditions, localization (5) is exact up to first order, and it is easy to demonstrate (Dagan, 1989, *ibid*) that, for any correlation function ρ_Y,

$$\hat{\mathbf{A}}^{(1)} = \frac{\sigma_Y^2}{d} \mathbf{I}, \tag{12}$$

where d is the space dimension. It then follows from Equation (11) that apparent transmissivity of a medium is, in fact, an effective property and is given (up to first order in σ_Y^2) by a scalar $T_{ef}^{[1]} \equiv T_{ef}^{(0)} + T_{ef}^{(1)} = T_g[1 + (1/2 - 1/d)\sigma_Y^2]$. This gives rise to apparent transmissivities given by harmonic, $T_{ef} = T_h = \exp(-\sigma_Y^2/2)$, and geometric, $T_{ef} = T_g$, means for one- ($d = 1$) and two- ($d = 2$) dimensional flows, respectively. Since most analyses of apparent parameters dealt with infinite domains (e.g. Indelman *et al.*, 1996 and references therein), the tensorial nature of these parameters remains to a large extent unexplored.

Flow domain's boundary affects apparent parameters in two interconnected ways: through its presence *per se*, and through a type of boundary conditions. Specifically, the presence of boundaries leads to $\nabla \bar{h}^{(1)} \neq 0$, so that, in general, the localization alone does not lead to apparent transmissivity. For relatively simple flow

scenarios, numerical simulations of Guadagnini and Neuman (1999a, b) demonstrated that $\nabla\bar{h}^{(1)} \ll \nabla\bar{h}^{(0)}$ throughout most of the flow domain. For such flow conditions, it might be possible to neglect $\nabla\bar{h}^{(1)}$ and to treat the term in the square brackets in Equation (11) as the first-order approximation of apparent transmissivity. This approximation was used by Paleologos *et al.* (1996), Tartakovsky and Neuman (1998c), and by Indelman *et al.* (1996), among many others.

However, for more general flow conditions (e.g. in the presence of singularities caused by pumping or injection wells), $\nabla\bar{h}^{(1)}$ can be at least of the same order as $\nabla\bar{h}^{(0)}$ (Guadagnini and Neuman, 1999b). Moreover, at these locations the mean uniform flow approximation becomes invalid. These observations render the standard approximation of apparent transmissivity inadequate.

We generalize the standard first-order approximation of apparent (effective) transmissivity by noting that, after localization

$$\nabla\bar{h}^{(1)} \approx \mathcal{T}\left(-\frac{\sigma_Y^2}{2}\mathbf{I} + \hat{\mathbf{A}}^{(1)}\right)\mathbf{J}, \tag{13a}$$

where the tensor $\mathcal{T}$ is given by

$$\mathcal{T}(\mathbf{x}) = \int_\Omega \nabla_{\mathbf{x}}\nabla_{\mathbf{y}}^T G(\mathbf{y}, \mathbf{x})\, d\mathbf{y}. \tag{13b}$$

Then the up to first-order approximation of the apparent transmissivity tensor is

$$\mathbf{T}_{ap}^{[1]}(\mathbf{x}) = \mathbf{T}_{ap}^{(0)} + \mathbf{T}_{ap}^{(1)}(\mathbf{x}) \tag{14a}$$

with

$$\mathbf{T}_{ap}^{(0)} = T_g\mathbf{I} \quad \text{and} \quad \frac{\mathbf{T}_{ap}^{(1)}(\mathbf{x})}{T_g} = \mathcal{T}\left(-\frac{\sigma_Y^2}{2}\mathbf{I} + \hat{\mathbf{A}}^{(1)}\right) + \frac{\sigma_Y^2}{2}\mathbf{I} - \hat{\mathbf{A}}^{(1)}(\mathbf{x}). \tag{14b}$$

Since the tensors $\hat{\mathbf{A}}^{(1)}$ and $\mathcal{T}$ depend on the Green's function (8), the apparent transmissivity tensor (14) depends not only on the domain geometry but also on the type of boundary conditions, that is, on a flow regime.

We now proceed to investigate the properties of the apparent transmissivity tensor and to test accuracy of the underlying approximations.

4. Computational Example

Consider steady-state flow through a rectangular domain of length a and width b. The rectangle is embedded within a statistically homogeneous Gaussian log-transmissivity field Y with the isotropic separated-exponential correlation structure

$$\rho_Y(\mathbf{y}^*, \mathbf{x}^*) = \exp\left(-\frac{|y_1^* - x_1^*| + \epsilon|y_2^* - x_2^*|}{\lambda}\right). \tag{15}$$

Here $x_1^* = x_1/a$ ($y_1^* = y_1/a$) and $x_2^* = x_2/b$ ($y_2^* = y_2/b$) are the dimensionless coordinates, $\epsilon = b/a$, and $\lambda = l_Y/a$, where l_Y is the correlation scale. Constant heads, H_1 and H_2, are prescribed along the boundaries $x_1^* = 0$ and $x_1^* = 1$, respectively; while the other two boundaries, $x_2^* = 0$ and $x_2^* = 1$, are assumed impermeable, $\partial h/\partial x_2^* = 0$.

The Green's function, G, is now given by

$$G(\mathbf{y}^*, \mathbf{x}^*) \;=\; \frac{2}{\pi} \sum_{n=1}^{\infty} \frac{1}{n \,\sinh(\pi\epsilon n)} \,\sin(\pi n y_1^*)\, \sin(\pi n x_1^*)\, \gamma_n(y_2^*, x_2^*), \qquad (16a)$$

where

$$\gamma_n(y_2^*, x_2^*) = \begin{cases} \cosh(\pi\epsilon n y_2^*) \cosh(\pi\epsilon n[x_2^* - 1]), & 0 \leqslant y_2^* \leqslant x_2^* \\ \cosh(\pi\epsilon n[y_2^* - 1]) \cosh(\pi\epsilon n x_2^*), & x_2^* \leqslant y_2^* \leqslant 1. \end{cases} \qquad (16b)$$

This Fourier series representation of the Green's function, and especially its second derivatives, are known to convergence slowly. This makes direct use of (16) for numerical computations impractical (Tartakovsky and Mitkov, 1999). We improve convergence of this series in Appendix.

4.1. AN ANALYTICAL SOLUTION

We start by evaluating in Appendix tensors $\hat{\mathbf{A}}^{(1)}$ and $\mathcal{T}$ given by (8) and (13b), respectively. The resulting apparent transmissivity tensor (14) spans the two-parameter space of the shape factor ϵ and relative correlation length λ. Its components have the following asymptotic behavior. For $\epsilon \to 0$ and finite λ

$$\frac{\hat{A}_{11}^{(1)}}{\sigma_Y^2} = 1 + \lambda \left[\exp\left(-\frac{x_1^*}{\lambda}\right) + \exp\left(-\frac{1 - x_1^*}{\lambda}\right) - 2 \right], \qquad \frac{\hat{A}_{22}^{(1)}}{\sigma_Y^2} = 1 \qquad (17)$$

and $\hat{A}_{12}^{(1)} = \hat{A}_{21}^{(1)} = 0$.

For $\epsilon \to \infty$ and finite λ

$$\begin{aligned} \frac{\hat{A}_{11}^{(1)}}{\sigma_Y^2} \;&=\; 1 + \lambda \left[\exp\left(-\frac{x_1^*}{\lambda}\right) + \exp\left(-\frac{1 - x_1^*}{\lambda}\right) - 2 \right] - \\ &\quad - 2\lambda \sum_{n=1}^{\infty} \frac{2\cos(\pi n x_1^*) - \xi(n, x_1^*)}{(1 + \pi^2\lambda^2 n^2)(1 + \pi\lambda n)} \cos(\pi n x_1^*), \\ \frac{\hat{A}_{22}^{(1)}}{\sigma_Y^2} \;&=\; 2\lambda \sum_{n=1}^{\infty} \frac{2\sin(\pi n x_1^*) + \xi(n+1, x_1^*)}{(1 + \pi^2\lambda^2 n^2)(1 + \pi\lambda n)} \sin(\pi n x_1^*), \end{aligned} \qquad (18)$$

and $\hat{A}_{12}^{(1)} = \hat{A}_{21}^{(1)} = 0$. Here

$$\xi(n, x_1^*) = \exp\left(-\frac{x_1^*}{\lambda}\right) + (-1)^n \exp\left(\frac{x_1^* - 1}{\lambda}\right). \qquad (19)$$

For $\lambda \to 0$ and finite ϵ

$$\frac{\hat{A}_{11}^{(1)}}{\sigma_Y^2} = \frac{\hat{A}_{22}^{(1)}}{\sigma_Y^2} = \frac{1}{2} \quad \text{and} \quad \hat{A}_{12}^{(1)} = \hat{A}_{21}^{(1)} = 0. \tag{20}$$

For $\lambda \to \infty$ and finite ϵ

$$\begin{aligned}
\frac{\hat{A}_{11}^{(1)}}{\sigma_Y^2} &= 0, \\
\hat{A}_{12}^{(1)} &= \frac{4}{\pi} \sum_{n=1,3}^{\infty} \frac{\cos(\pi n x_1^*)}{n} \frac{\cosh(\pi \epsilon n x_2^*) - \cosh[\pi \epsilon n (x_2^* - 1)]}{\sinh(\pi \epsilon n)}, \\
\frac{\hat{A}_{21}^{(1)}}{\sigma_Y^2} &= 0, \\
\frac{\hat{A}_{22}^{(1)}}{\sigma_Y^2} &= \frac{4}{\pi} \sum_{n=1,3}^{\infty} \frac{\sin(\pi n x_1^*)}{n} \frac{\sinh(\pi \epsilon n x_2^*) - \sinh[\pi \epsilon n (x_2^* - 1)]}{\sinh(\pi \epsilon n)}.
\end{aligned} \tag{21}$$

We further note that tensor $\sigma_Y^2 \mathcal{T}$ can be obtained from the tensor $\hat{\mathbf{A}}$ by taking the limit as $\lambda \to \infty$. Hence, the components of tensor $\sigma_Y^2 \mathcal{T}$ are given by Equation (21).

For intermediate values of the parameters ϵ and λ, analytic expressions for the first-order approximation of the apparent transmissivity tensor $\mathbf{T}_{ap}$ are more cumbersome. Instead of reproducing these expressions here, we plot them on Figures 1 and 2 for $\epsilon = 1$ (square domain) and $\lambda = 0.5$ and $\lambda = 0.05$, respectively. In the flow domain's interior, $\mathbf{T}_{ap}^{(1)}$ is diagonally-dominant. Its four components, $T_{ij}^{(1)}$, are symmetric with respect to the domain center, and $T_{ij}^{(1)} = 0$ ($i \neq j$ and $i = j = 2$) away from the domain boundaries. Ignoring tensor $\mathcal{T}$ leads to the non-symmetric apparent transmissivity tensor, which contradicts to the traditional definition of hydraulic conductivity or transmissivity (e.g. Bear, 1972, Equation 4.8.17). Incorporating $\mathcal{T}$ resolves this problem. (The fact that close to the boundaries $T_{ij}^{(1)} = 0$ ($i \neq j$) only approximately is due to perturbative nature of our solution.)

Figure 3 allows us to analyze spatial variation of the apparent transmissivity tensor in greater detail. It depicts the longitudinal cross-section, $x_2^* = 0.5$, of the diagonal components of $\mathbf{T}_{ap}^{(1)}$, normalized by $T_g \sigma_Y^2$, $\epsilon = 1$ and several values of λ. For 'subgrid' upscaling – when upscaling domains are smaller than correlation length of transmissivity, that is, $\lambda < 1$ – spatial variability of the apparent transmissivity tensor is persistent throughout the upscaling domain. When upscaling domain spans enough correlation lengths ($\lambda > 1$) this variability diminishes and it might be appropriate to replace $\mathbf{T}_{ap}^{[1]}(\mathbf{x})$ with a constant $\mathbf{T}_{ap}^{[1]}$ evaluated at the domain's center.

Figure 4 demonstrates the influence of parameters λ and ϵ on the apparent transmissivity tensor evaluated at the domain center, $x_1^* = x_2^* = 0.5$. As the domain size (relative to the correlation scale) increases, that is, $\lambda \to 0$, the longitudinal

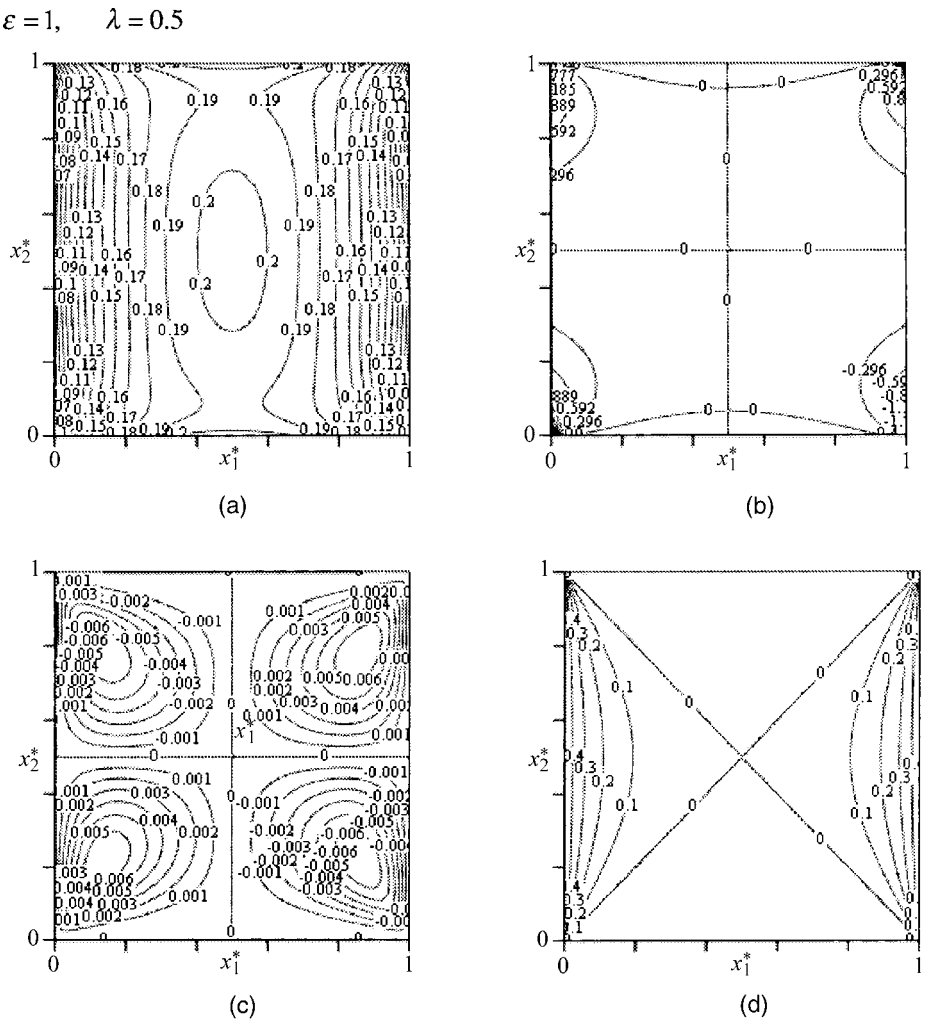

Figure 1. Four components of the second-rank tensor $\mathbf{T}_{ap}^{(1)}(\mathbf{x})/(T_g\sigma_Y^2)$, for $\epsilon = 1.0$ and $\lambda = 0.5$: (a) $T_{11}^{(1)}/(T_g\sigma_Y^2)$, (b) $T_{12}^{(1)}/(T_g\sigma_Y^2)$, (c) $T_{21}^{(1)}/(T_g\sigma_Y^2)$, and (d) $T_{22}^{(1)}/(T_g\sigma_Y^2)$.

component of the apparent transmissivity tensor tends to its well-established value $T_{11}^{(1)} \to 0$. The same holds for the transverse component of the apparent transmissivity tensor, $T_{22}^{(1)}$, even though it approaches 0 at a different rate than $T_{11}^{(1)}$ does and the boundary effects are more persistent close to the boundaries (Figure 3). Although not shown here, throughout the upscaling domain the off-diagonal terms $T_{12}^{(1)}$ and $T_{21}^{(1)} \to 0$ as $\lambda \to 0$.

Thus, when $\lambda \to 0$ and the flow domain remains essentially two-dimensional, that is, spans over a sufficient number of correlation scales in the x_1 and x_2 directions, apparent transmissivity is given by a scalar, the geometric mean of local transmissivity, T_g. For practical purposes, this occurs for domains as large as

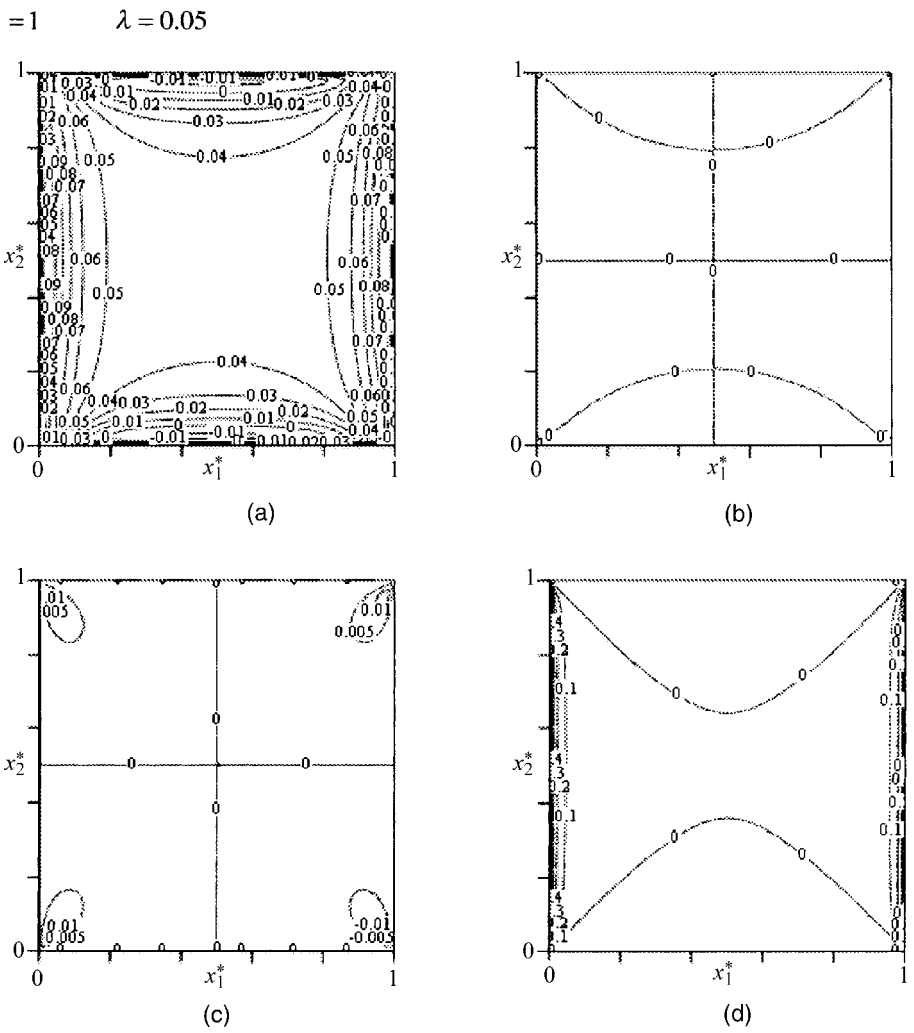

Figure 2. Four components of the second-rank tensor $\mathbf{T}_{ap}^{(1)}(\mathbf{x})/(T_g\sigma_Y^2)$, for $\epsilon = 1.0$ and $\lambda = 0.05$: (a) $T_{11}^{(1)}/(T_g\sigma_Y^2)$, (b) $T_{12}^{(1)}/(T_g\sigma_Y^2)$, (c) $T_{21}^{(1)}/(T_g\sigma_Y^2)$, and (d) $T_{22}^{(1)}/(T_g\sigma_Y^2)$.

$\lambda = 0.02$. Boundary and geometrical effects become more persistent as λ increases.

There are two well-established asymptotic limits of effective (apparent) transmissivity, which correspond to flow through perfectly stratified media in the directions either parallel or perpendicular to stratification (e.g. Dagan, 1989, Eq. 3.4.62). These limits are readily recovered from our expressions. Indeed, one can see from our asymptotic relations for the apparent transmissivity tensor that for $\lambda > 1$, both $T_{11}^{(1)}/(T_g\sigma_Y^2)$ and $T_{22}^{(1)}/(T_g\sigma_Y^2)$ tend to 0.5 (and $T_{12}^{(1)} = T_{21}^{(1)} = 0$) as ϵ increases. These conditions correspond to flow parallel to stratification and, not surprisingly, apparent transmissivity tends to the arithmetic mean of local transmissivity, T_a.

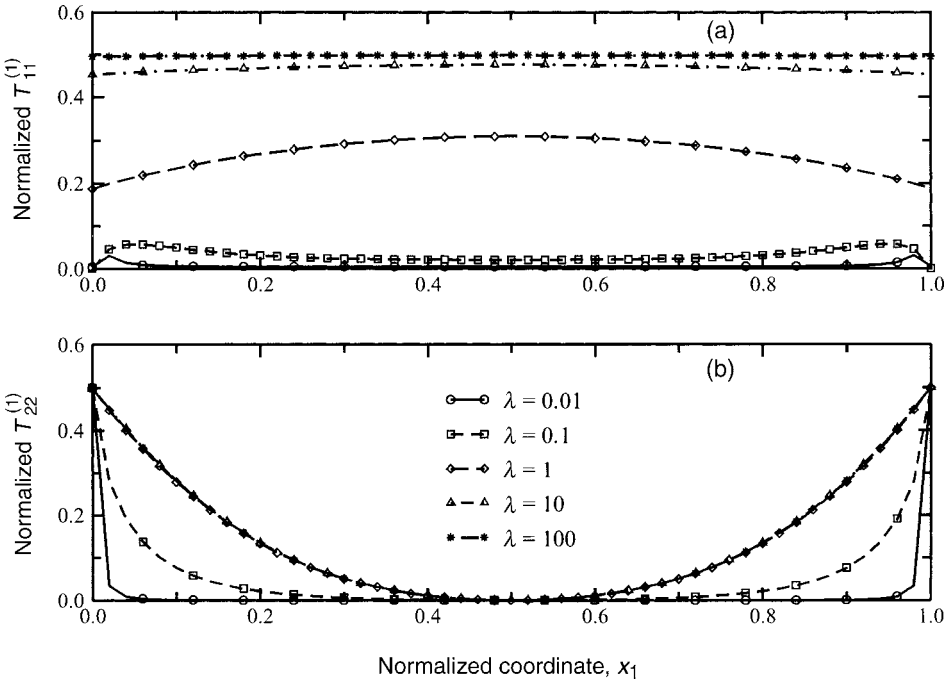

Figure 3. Longitudinal cross-section, $x_2^* = 0.5$, of (a) $T_{11}^{(1)}$ and (b) $T_{22}^{(1)}$, normalized by $T_g\sigma_Y^2$, for $\epsilon = 1$ and several values of λ.

By the same token, one can see that $T_{11}^{(1)}/(T_g\sigma_Y^2) \to -0.5$ and $T_{22}^{(1)} \to 0$ as both ϵ and λ tend to 0. This limit corresponds to essentially one-dimensional flow. In agreement with previous findings, $\mathbf{T}_{ap} \to T_h$, the harmonic mean of local transmissivity.

4.2. LOCALIZATION EFFECTS

Our expression (14) for apparent transmissivity, $\mathbf{T}_{ap}^{[1]}$, is based on the assumption that flow is either uniform in the mean ($\nabla\bar{h} = \text{const}$), or varies slowly in space. To investigate the robustness of this assumption, we place a pumping well at the the center of the rectangular flow domain considered in the previous section. Clearly, this results in non-uniform flow close to the well. Similar flow problems were recently investigated analytically (Guadagnini and Tartakovsky, 2000) and numerically (Guadagnini and Neuman, 1999b; Neuman and Guadagnini, 1999).

We consider a square flow domain with $a = b = 10$. As before, the square is embedded within a statistically homogeneous Gaussian field of log transmissivity. It is now assumed that the geometric mean $T_g = 1$, correlation scale $l_Y = 1$, and variance $\sigma_Y^2 = 1$. Constant heads $H_1 = 15$ and $H_2 = 5$ are prescribed along the boundaries $x_1 = 0$ and $x_1 = a$, respectively. The pumping well is located at $x_1 = x_2 = a/2$ and operates at a constant rate $Q = 1$.

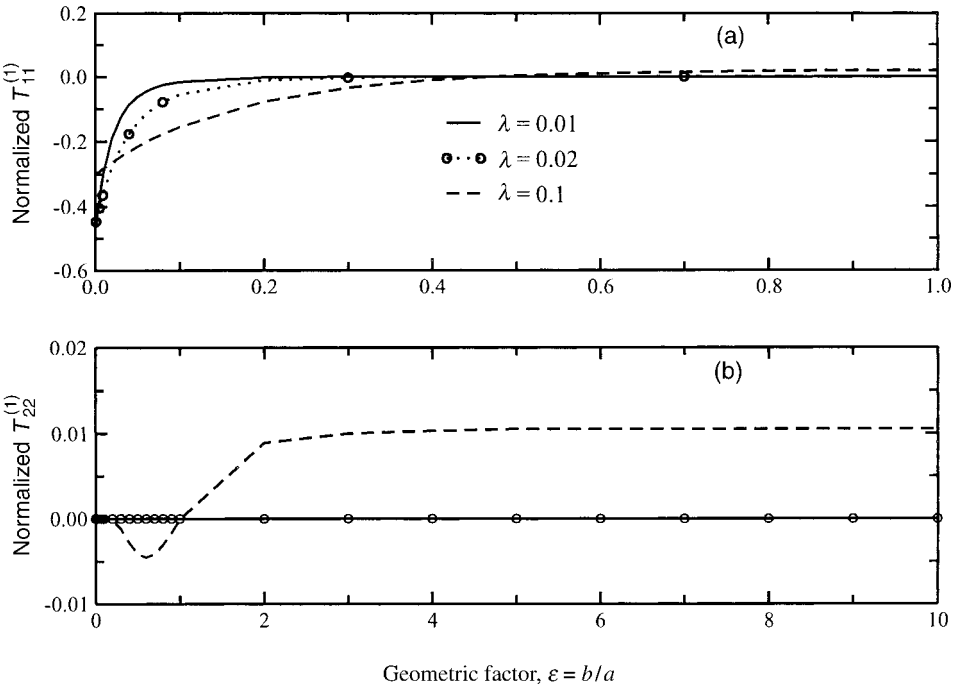

Figure 4. Dependence of (a) $T_{11}^{(1)}$ and (b) $T_{22}^{(1)}$ on the domain geometry, ϵ, for several values of λ. Both $T_{11}^{(1)}$ and $T_{22}^{(1)}$ are normalized by $T_g \sigma_Y^2$ and evaluated at the domain center, $x_1^* = x_2^* = 0.5$.

We compare the mean head distributions, $\bar{h}$, resulting from four alternative approaches:

(i) localization of the nonlocal mean flow equations that leads to our apparent transmissivity tensor, $\bar{h}_{LE}$;
(ii) numerical solution of the first-order approximation of the nonlocal mean flow equations, $\bar{h}_{ME}$;
(iii) numerical solution of deterministic flow equations for the uniform medium of transmissivity T_g (Neuman and Guadagnini, 1999), $\bar{h}_{MF}$; and
(iv) Monte-Carlo simulations, $\bar{h}_{MC}$.

The nonlocal mean flow equations are solved by Galerkin finite elements (Guadagnini and Neuman, 1999a, b) on rectangular grid with 2500 square elements (50 rows by 50 columns) of uniform size $\triangle x_1 = \triangle x_2 = 0.2$. Our analytical expression for the apparent conductivity tensor is evaluated at the element centers and these values are assigned to the corresponding elements. Monte-Carlo simulations employ 3000 unconditional realizations of log transmissivity generated by means of the Gaussian sequential simulator SGSIM (Deutsch and Journel, 1992) on the same grid.

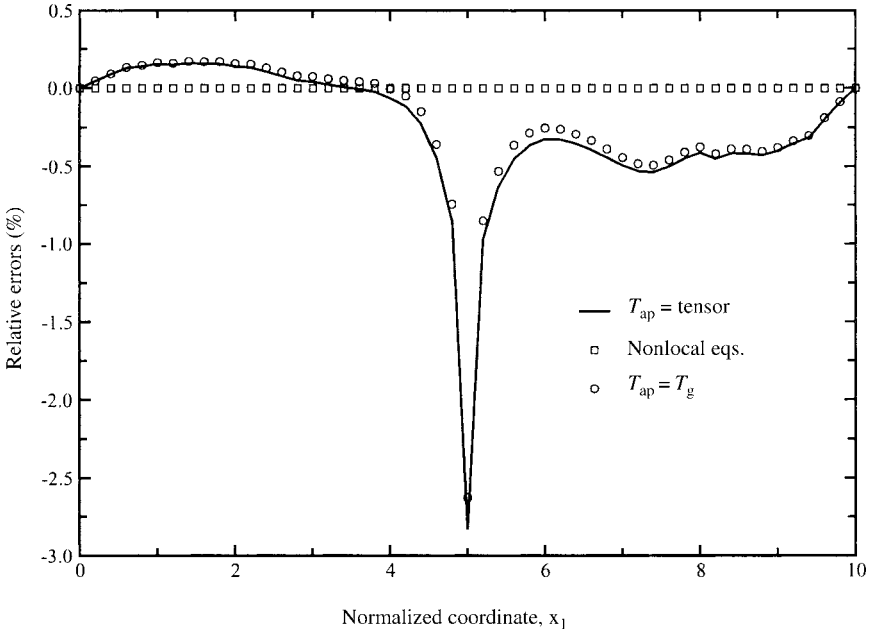

Figure 5. Relative errors in mean hydraulic head computed with the apparent transmissivity tensor (solid line), the nonlocal moment equations (squares), and the mean field approximation (circles).

Following standard practice in groundwater hydrology, we treat the solution based on Monte-Carlo simulations, $\bar{h}_{MC}$, as the 'ground truth'. Then accuracy of the three alternative approximations (i)–(iii) can be expressed in terms of the relative errors, $\mathcal{E}_i = (\bar{h}_{MC} - \bar{h}_i)/\bar{h}_{MC} \times 100\%$, where $i = LE, ME$, and MF. Figure 5 depicts the longitudinal cross-section, $x_2 = b/2$, of $\mathcal{E}_i$. The solutions obtained by solving the nonlocal mean flow equations, $\bar{h}_{ME}$, and from Monte-Carlo simulations, $\bar{h}_{MC}$ practically coincide. Throughout the flow domain, the solution, $\bar{h}_{LE}$, based on $\mathbf{T}_{ap}$ slightly over-estimates the 'actual' head distribution and practically coincides with the mean field solution (Guadagnini and Neuman, 1999b; Neuman and Guadagnini, 1999) based on the geometric mean of transmissivity. Not surprisingly, the largest errors occur in the vicinity of the well where the head gradients are expected to be large.

As expected, localization errors, $\mathcal{E}_{LE}$, increase with increasing pumping rates at the well (Table I). Somewhat more surprising is that geometric mean of transmissivity yields more accurate estimate of mean head than apparent transmissivity does. Since our expressions are derived through perturbation expansions in small parameter $\sigma_Y^2 \ll 1$, it should come as no surprise that their quality deteriorates with increasing σ_Y^2. Nevertheless, the mean head estimates remain relatively robust for moderately large σ_Y^2. To sum up, despite the disagreement between the nonlocal and localized solutions, it might be feasible to rely on the concept of apparent trans-

Table I. Relative errors $\mathcal{E}_{LE}$ and $\mathcal{E}_{MF}$ in the mean hydraulic heads computed using the apparent transmissivity tensor and the mean field approximation, respectively

Pumping rate, Q	Variance, σ_Y^2	Error $\lvert\mathcal{E}_{LE}\rvert$	Error $\lvert\mathcal{E}_{MF}\rvert$
1.0	1.0	2.83	2.62
100.0	1.0	22.33	20.59
1.0	2.0	6.30	6.09
100.0	2.0	38.68	37.31
1.0	4.0	17.93	17.70
100.0	4.0	64.19	63.39

missivity when the medium is moderately heterogeneous and the high resolution is not crucial.

5. Discussion

Our analysis is founded on the premise that all quantities (parameters, state variables, and forcing terms) in flow equations are measurable, or can be deduced from measurements, on some consistent support scale ω at any point $\mathbf{x}$. Transmissivity is treated as a multivariate random field with a well-defined geostatistical structure. This renders hydraulic heads and fluxes random.

One way to solve stochastic ω-scale flow equations is numerically by means of conditional/unconditional Monte-Carlo simulations. Ideally, such simulations should be conducted on a computational grid with fine ω-scale space discretization, so as to allow resolving all spatial frequencies of the corresponding ω-scale random functions that may manifest themselves within the flow domain. If these frequencies are low enough to extend across much of the flow domain, as is the case with random fractals, the simulations should be conducted on grids that are considerably larger than flow domains. When these computationally demanding conditions are satisfied, each Monte-Carlo realization produces a realistically looking space-time image of ω-scale hydraulic heads and fluxes at a high resolution of scale ω.

When space-time images of ω-scale hydraulic heads and fluxes are averaged in the Monte-Carlo process, their random ω-scale fluctuations are smoothed out. The resulting averages represent smoothed versions of the reality. For example, the averaged flux $\bar{\mathbf{q}}(\mathbf{x})$ no longer represents a likely realization of ω-scale flux $\mathbf{q}$ at the point $\mathbf{x}$ in space, but its ensemble average. Though the estimator $\bar{\mathbf{q}}(\mathbf{x})$ is smoother than its real (random) counterpart $\mathbf{q}$, it is still defined on the scale ω. No spatial averaging, or upscaling, of any sort is used in the calculation of $\bar{\mathbf{q}}(\mathbf{x})$; the averaging is done solely in the probability space, across realizations.

In this paper we use a local (dependent on only one point in space and time) parameter $\bar{T}(\mathbf{x})$, which represents an optimum unbiased estimator of transmissivity $T(\mathbf{x})$. As such, $\bar{T}(\mathbf{x})$ is not a spatially averaged or upscaled version of $T(\mathbf{x})$, but

rather is its probabilistic average defined on the scale ω. While random realizations of unknown transmissivity $T(\mathbf{x})$ might provide realistically looking images of transmissivity with a spatial resolution ω, $\bar{T}$ provides their probabilistically smoothed average with the same spatial resolution. In these cases one can define space-dependent apparent transmissivity $\mathbf{T}_{ap}(\mathbf{x})$. This parameter also varies with the domain size.

On the basis of our interpretation, it is clear that force-fitting a traditional deterministic model to measured ω-scale hydraulic heads and fluxes, implies treating these data as if they represented their estimators $\bar{h}$ and $\bar{\mathbf{q}}$, respectively. Such a fit returns a tensor that is closely related to $\mathbf{T}_{ap}(\mathbf{x})$. Hence, its magnitude appears to vary with the domain size and the scale of measurements. Since there is always uncertainty about local (ω-scale) heterogeneities, a deterministic analysis of flow is never warranted unless the flow model is viewed and interpreted in the manner just described.

6. Conclusions

Our analysis of apparent transmissivity leads to the following major conclusions:

1. We defined apparent transmissivity $\mathbf{T}_{ap}$ as the ratio between the ensemble means (estimators) of flux, $\bar{\mathbf{q}}$, and hydraulic head gradient, $\nabla\bar{h}$, that is, $\bar{\mathbf{q}} = -\mathbf{T}_{ap}\nabla\bar{h}$. In line with the previous findings, we demonstrated that apparent transmissivity is rigorously valid for mean uniform flows ($\nabla\bar{h} = \text{const}$) only. Otherwise, the mean flow equations are nonlocal, and it is necessary to assume that $\nabla\bar{h}$ and the residual (dispersive) flux $\mathbf{r}$ vary slowly in space.

2. If localization of the mean flow equations is feasible, then apparent transmissivity is given by a second-rank tensor. Tensorial nature of a general expression for $\mathbf{T}_{ap}$ is caused by the presence of the flow domain boundaries and occurs even for statistically isotropic transmissivity fields. The tensorial nature of apparent transmissivity implies that, while the estimator of hydraulic head gradient $\nabla\bar{h}$ is collinear to its random counterpart ∇h, the flux estimator $\bar{\mathbf{q}}$ has a different direction than $\mathbf{q}$.

3. Our general expression for the apparent transmissivity tensor requires a closure approximation to be workable. We derived such a closure through a perturbation expansion in σ_Y^2, the variance of log-transmissivity, $Y = \ln T$. We derived an analytical expression for $\mathbf{T}_{ap}^{[1]}$ of the rectangular flow domain. The apparent transmissivity tensor varies in space, with all four components being symmetric with respect to the rectangle center.

4. To investigate applicability of the apparent transmissivity tensor to nonuniform mean flows, we introduced a pumping well into the problem. The mean head distribution resulting from the use of apparent transmissivity was compared with those obtained from Monte-Carlo simulations, from nonlocal mean flow equations, and from deterministic flow equations with the geometric mean T_g. This comparison shows that reliance on the apparent transmissivity tensor over-estimates

the actual head distributions. The largest errors occur close to the well, where flow is strongly non-uniform. These errors increase with the pumping rate.

Appendix

In this Appendix we derive an alternative expression for the Green's function (16), which has a greatly improved rate of convergence. We then use this expression to calculate the components of tensors **A** and **B**.

We start by rewriting (16) as

$$G(\mathbf{y}^*, \mathbf{x}^*) = \frac{1}{\pi} \sum_{n=1}^{\infty} \frac{1}{n} \sin(\pi n y_1^*) \sin(\pi n x_1^*) \hat{\gamma}_n(y_2^*, x_2^*), \tag{22a}$$

where

$$\hat{\gamma}_n(y_2^*, x_2^*) = \frac{\cosh[\pi \epsilon n(y_2^* + x_2^* - 1)] + \cosh[\pi \epsilon n(|y_2^* - x_2^*| - 1)]}{\sinh(\pi \epsilon n)}. \tag{22b}$$

We further note that, for $n \to \infty$,

$$\hat{\gamma}_n(y_2^*, x_2^*) \to e^{-\pi \epsilon n |y_2^* - x_2^*|} + e^{-\pi \epsilon n (2 - y_2^* - x_2^*)}. \tag{23}$$

Adding and subtracting this limit from (22), and summing up the added part (Gradshteyn and Ryzhik, 1980, Eq. 1.462), yields

$$G(\mathbf{y}^*, \mathbf{x}^*) = G_1(\mathbf{y}^*, \mathbf{x}^*) + G_2(\mathbf{y}^*, \mathbf{x}^*), \tag{24a}$$

where the leading term

$$\begin{aligned} G_1 \;=\; & \frac{1}{4\pi} \ln \left[\frac{\sin^2(\pi(y_1^* + x_1^*)/2) + \sinh^2(\pi \epsilon (y_2^* - x_2^*)/2)}{\sin^2(\pi(y_1^* - x_1^*)/2) + \sinh^2(\pi \epsilon (y_2^* - x_2^*)/2)} \right] + \\ & + \frac{1}{4\pi} \ln \left[\frac{\sin^2(\pi(y_1^* + x_1^*)/2) + \sinh^2(\pi \epsilon (2 - y_2^* - x_2^*)/2)}{\sin^2(\pi(y_1^* - x_1^*)/2) + \sinh^2(\pi \epsilon (2 - y_2^* - x_2^*)/2)} \right] \end{aligned} \tag{24b}$$

contains the singularity and the second term

$$\begin{aligned} G_2 \;=\; & \frac{1}{\pi} \sum_{n=1}^{\infty} \frac{\sin(\pi n y_1^*) \sin(\pi n x_1^*)}{n} \times \\ & \times [\hat{\gamma}_n - e^{-\pi \epsilon n |y_2^* - x_2^*|} - e^{-\pi \epsilon n (2 - y_2^* - x_2^*)}] \end{aligned} \tag{24c}$$

is an exponentially convergent series.

Substituting (15) and (22) into (8) gives $\hat{A}_{ij}^{(1)}$, the four components of the second-rank tensor $\hat{\mathbf{A}}^{(1)}$.

Acknowledgements

This work was performed under the auspices of the U.S. Department of Energy (DOE), DOE/BES (Bureau of Energy Sciences) Program in the Applied Mathematical Sciences Contract KC-07-01-01. Partial support is due to the European Commission under Contract No. EVK1-CT-1999-00041 (W-SAHARA – Stochastic Analysis of Well Protection and Risk Assessment).

References

Bear, J.: 1972, *Dynamics of Fluids Porous Media*, Elsevier, New York.

Cushman, J.: 1997, *The Physics of Fluids in Hierarchical Porous Media: Angstroms to Miles*, Kluwer Academic Publisher, New York.

Dagan, G.: 1982, Analysis of flow through heterogeneous random aquifers. 2. Unsteady flow in confined formations, *Water Resour. Res.* **18**(5), 1571–1585.

Dagan, G.: 1989, *Flow and Transport in Porous Formations*, Springer-Verlag, New York.

Deutsch, C. V. and Journel, A. G.: 1992, *Geostatistical Software Library and User's Guide*, Oxford University Press, New York.

Gelhar, L. W.: 1993, *Stochastic Subsurface Hydrology*, Prentice Hall, New Jersey.

Gradshteyn, I. S. and Ryzhik, I. M.: 1980, *Table of Integrals, Series, and Products*, Academic Press, New York.

Guadagnini, A. and Neuman, S. P.: 1999a, Nonlocal and localized analyses of conditional mean steady state flow in bounded, randomly nonuniform domains. 1. Theory and computational approach, *Water Resour. Res.* **35**(10), 2999–3018.

Guadagnini, A. and Neuman, S. P.: 1999b, Nonlocal and localized analyses of conditional mean steady state flow in bounded, randomly nonuniform domains. 2. Computational examples, *Water Resour. Res.* **35**(10), 3019–3040.

Guadagnini, A. and Tartakovsky, D. M.: 2000, Stochastic analysis of groundwater pumping from bounded, randomly heterogeneous aquifers, in: D. Zhang and C. L. Winter (eds), *Theory, Modeling, and Field Investigation in Hydrology: A GSA Special Volume in Honor of Shlomo P. Neuman's 60th Birthday (Geological Society of America Special Paper 348)*, pp. 73–79.

Indelman, P., Fiori, A. and Dagan, G.: 1996, Steady flow toward wells in heterogeneous formations: mean head and equivalent conductivity, *Water Resour. Res.* **32**(7), 1975–1983.

Matheron, G.: 1967, Composition de perméabilité en milieu poreux hétérogène: Méthode de Schwydler règles de pondération, *Revue de l'IFP (Rev. Inst. Fr. Pet.)* **22**, 443–466.

Neuman, S. P.: 1994, Generalized scaling of permeabilities: validation and effect of support scale, *Geophys. Res. Lett.* **21**(5), 349–352.

Neuman, S. P. and Guadagnini, A.: 1999, A new look at traditional deterministic flow models and their calibration in the context of randomly heterogeneous media, in: *Proceedings International Conference on Calibration and Reliability in Groundwater Modeling, ModelCARE-99*, Vol. 1, Zurich, Switzerland, pp. 189–197.

Neuman, S. P. and Orr, S.: 1993, Prediction of steady state flow in nonuniform geologic media by conditional moments: exact nonlocal formalism, effective conductivities, and weak approximation, *Water Resour. Res* **29**(2), 341–364.

Neuman, S. P., Tartakovsky, D. M., Wallstrom, T. C. and Winter, C. L.: 1996, Correction to the Neuman and Orr 'Nonlocal theory of steady state flow in randomly heterogeneous media', *Water Resour. Res.* **32**(5), 1479–1480.

Paleologos, E. K., Neuman, S. and Tartakovsky, D. M.: 1996, Effective hydraulic conductivity of bounded, strongly heterogeneous porous media, *Water Resour. Res.* **32**(5), 1333–1341.

Sànchez-Vila, X.: 1997, Radially convergent flow in heterogeneous porous media, *Water Resour. Res.* **33**(7), 1633–1641.

Tartakovsky, D. M., Guadagnini, A. and Guadagnini, L.: 2000, Effective hydraulic conductivity and transmissivity for heterogeneous aquifers, *Math. Geol.* **32**(6), 751–759.

Tartakovsky, D. M., Guadagnini, A. and Riva, M.: 1999, Stochastic analysis of effective conductivity in bounded, randomly heterogeneous aquifers with pumping, in: *Proceedings of the 5th Annual Conference of the International Association for Mathematical Geology (IAMG99)*, Vol. II, Trondheim, Norway, pp. 760–766.

Tartakovsky, D. M. and Mitkov, I.: 1999, Some aspects of head-variance evaluation, *Comp. Geosci.* **3**(1), 89–92.

Tartakovsky, D. M. and Neuman, S. P.: 1998a, Transient effective hydraulic conductivities under slowly and rapidly varying mean gradients in bounded three-dimensional random media, *Water Resour. Res.* **34**(1), 21–32.

Tartakovsky, D. M. and Neuman, S. P.: 1998b, Transient flow in bounded randomly heterogeneous domains. 1. Exact conditional moment equations and recursive approximations, *Water Resour. Res.* **34**(1), 1–12.

Tartakovsky, D. M. and Neuman, S. P.: 1998c, Transient flow in bounded randomly heterogeneous domains. 2. Localization of conditional mean equations and temporal nonlocality effects, *Water Resour. Res.* **34**(1), 13–20.